

Characterization of microstructural evolution during reverse transformation in a tempered martensite low-alloy steel

T. Shinozaki^{1*}, Y. Tomota², S. Harjyo³, W. Gong^{3,4}

¹ Steel Casting and Forging Division, Kobe Steel, Ltd., 2-3-1 Shinhama, Arai-cho, Takasago, Hyogo, 676-8670, Japan

² Research Center for Structure Materials, National Institute for Materials Science, 1-2-1 Sengen, Tsukuba, Ibaraki, 305-0047, Japan

³ J-PARC Center, Japan Atomic Energy Agency, 2-4 Shirane Shirakata, Tokai-mura, Naka-gun, Ibaraki, 319-1195, Japan

⁴ Elements Strategy Initiative for Structural Materials, Kyoto University, Yoshida-honmachi, Sakyo-ku, Kyoto, 606-8501, Japan

Abstract: Microstructure evolution during the reverse transformation of a Cr-Ni-Mo steel consisting of tempered lath martensite was examined using *in-situ* electron backscatter diffraction and neutron diffraction at high temperatures. Austenite grains nucleated during the reverse transformation were categorized into two types: austenite grains nucleated along the lath boundaries with almost the same crystal orientation (type A), and austenite grains nucleated at the prior austenite grain boundaries etc. with a different crystal orientation (type B). After the reverse transformation was finished, the prior austenite grains were reconstructed by the rapid growth and coalescence of type A grains, which was called the “austenite memory phenomenon.” Type A grains were characterized by high kernel average misorientation (KAM) values. Here, sub-boundaries remaining in such a reconstructed austenite grain original stemmed from the small-angle lath-boundaries of martensite. Hence, upon heating to a higher temperature, type A grains were invaded and were eventually replaced by type B grains, resulting in a new fine-grained polygonal microstructure; this was similar to recrystallization behavior. Therefore, these results showed that the austenite grain memory phenomenon occurred when the nucleation and growth of type A grains was more dominant than those of type B grains and that the degree of grain refinement depended on the nucleation and growth rate of the type B grains.

1. INTRODUCTION

Reverse transformation from ferrite (α) to austenite (γ) is often used to refine the grain size in the steel production process. However, the γ grain size after the γ reversion in bainitic or martensitic steel sometimes becomes as large as that of the previous γ , which is called “ γ memory” [1]. Interestingly, this reversed austenite with coarse grains changes to smaller grains at a much high-temperature annealing [2]. Numerous studies have already been conducted in an attempt to understand these phenomena [1-8]. The possibility of displacive (martensitic) transformation has been discussed when using iron-nickel alloys like maraging steel and/or a high heating rate. Such conditions are not applicable to the reverse transformation occurring at a slow heating rate in low-alloy steel, hence, other mechanisms should be discussed. The grain refining behavior that occurs after reverse transformation has been poorly investigated. One of the reasons for this is the fact that conventional microstructure observation techniques cannot reveal the characteristics of γ in low-alloy steel at elevated temperatures. In this study, microstructure evolution during the reverse transformation of a Cr-Ni-Mo steel consisting of tempered lath martensite at a slow heating rate was monitored by means of *in-situ* electron backscatter diffraction (EBSD) and *in-situ* neutron diffraction to clarify the mechanism for γ memory and grain refining behavior.

2. EXPERIMENTAL PROCEDURES

The steel used in this study was melted in a vacuum induction furnace and cast as 20 kg ingots. The

* Corresponding author. E-mail: shinozaki.tomoya@kobelco.com, telephone: +81 79 445 7198.

chemical composition of the steel was 0.36C-0.22Si-0.79Mn-0.007P-0.003S-3.04Cr-1.46Ni-0.43Mo-0.1V-0.03Al (in mass %) and balanced Fe. The ingots were forged into 40 mm square billets, from which 20 mm cubic specimens were machined. The specimens were annealed at 1453 K for 3.6 ks, followed by quenching in water. The quenched specimens were tempered at 973 K for 54 ks with the aim of precipitating the alloy carbides and decomposing the retained γ . The A_{C1} and A_{C3} temperatures determined by dilatometry were 1003 K and 1088 K, respectively.

In-situ EBSD measurements during annealing were carried out using a field emission (FE)-SEM with a heating stage (TSL solutions Co., Ltd.; HSEA-1000). A plate specimen that was $5 \times 7 \times 0.7$ (mm³) in size was cut from the quenched and tempered specimens. In this experiment, the temperature was increased in steps to obtain EBSD patterns at various temperatures from 973 to 1173 K with a heating rate of 0.05 K/s. The EBSD measurements were performed in a 400 μ m square region with a step size of 1 μ m during an isothermal holding of 2 ks. The obtained EBSD patterns were analyzed using an OIM system (EDAX Inc.; TSL OIM Analysis ver.7.2.1).

In-situ neutron diffraction measurements were performed during the heat treatment using a time-of-flight (TOF) neutron diffractometer, TAKUMI, at the Materials and Life Science Facility (MLF) in the Japan Proton Accelerator Research Complex (J-PARC). A cylindrical specimen 8 mm in diameter and 30 mm in length was prepared. The specimen was heated at a heating rate of 1 K/s from RT to 993 K (before the start of reverse transformation) and held there for 1.2 ks, then heated up to 1048 K at 0.05 k/s and held there for 1.2 ks, then to 1193 K (after the completion of γ reverse transformation), 1143 K, and finally 1223 K, in that order.

3. RESULTS AND DISCUSSION

3.1. *In-situ* SEM/EBSD observation of reverse transformation during annealing

Fig. 1 shows the results of *in-situ* SEM/EBSD measurements during annealing at several temperatures. A fully tempered martensitic structure with no retained γ was observed at 973 K (see in Fig. 1(a) and (c)). When the specimen was heated to 1048 K, the γ phase was detected by the EBSD measurement. The phase fraction of γ in Fig. 1(d) is approximately 51 %, which is in good agreement with the results determined using dilatometry. The reversed γ grains that nucleated along the lath boundaries have almost the same crystal orientation (type A). Additionally, a small number of fine γ grains with different crystal orientations (type B) nucleated at the prior γ grain boundaries and/or inside the prior γ grains as indicated by white arrows in Fig. 1(b).

Fig. 2(a) and (b) show IPF maps obtained at 1148 K and 1173 K, respectively. The reverse transformation had already been completed at temperatures below 1148 K. As can be seen in Fig. 2(a), reversed γ grains with a specific crystal orientation were mainly produced, and eventually constituted a γ grain of the same size as the prior γ grains. Then, with further reheating to 1173 K, some polygonal grains with different crystal orientations were produced and replaced the coarse grains. These behaviors are more obvious in the Kernel average misorientation (KAM) map. Fig. 2(c) and (d) show KAM maps for γ obtained at 1148 K and 1173 K, respectively. It is found that there are large KAM values within the coarse γ grains, immediately after the completion of the reverse transformation, whereas the fine grains indicated by the white arrows in Fig. 2(c) have a low KAM value. The lower region with the low KAM value shown

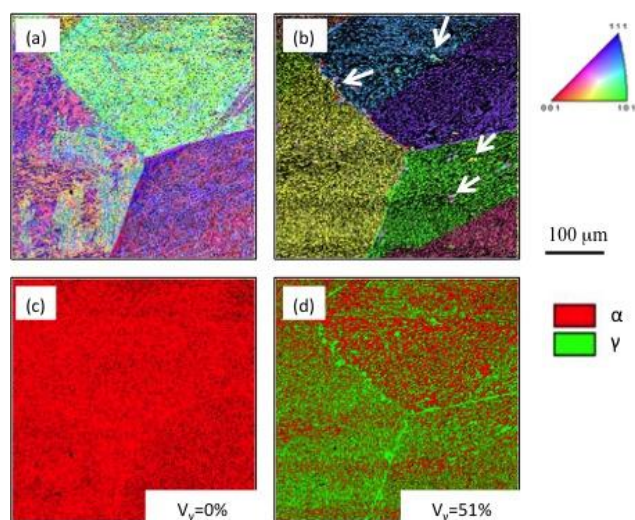


Fig.1 SEM/EBSD images obtained during annealing:
(a) Inverse pole figure (IPF) map of α . (b) IPF maps of γ . (c, d) Phase maps. (a, c) at 973 K, (b, d) at 1048 K.

in Fig. 2(d) corresponds to the newly apparent polygonal grains shown in Fig. 2(b), whereas the upper region with the high KAM value in Fig. 2(d) corresponds to the previously transformed grains, colored blue and violet in Fig. 2(a) and (b). An island region with a high KAM value in the middle of Fig. 2(d) was found to not appear newly but instead mixed with the former violet grains and invading red and blue polygonal grains. Some of the polygonal grains observed in Fig. 2(b) do not correspond to the tiny grains in Fig. 2(a) (see white arrows). Such new polygonal grains are thought to appear on the surface with the growth of those grains that have nucleated in the interior of the specimen. Those grains with a low KAM value correspond to type B grains with different crystal orientations. When the specimen was reheated at 1173 K, the coarse γ grains reconstructed by the growth of type A grains were gradually invaded and replaced by some grains with a low KAM value (see Fig. 2(d)). As a result, a new small grain structure was formed at a temperature higher than A_{C3} .

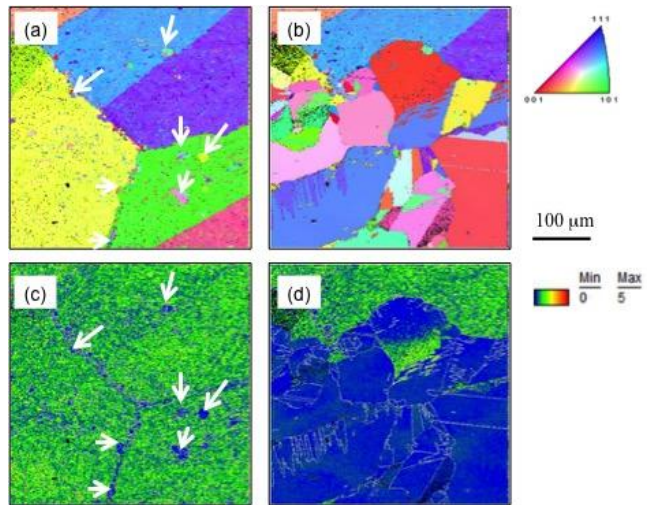


Fig.2 SEM/EBSD images obtained during annealing: (a, c) at 1148 K and (b, d) at 1173 K (b, d). (a) and (b) IPF maps of γ . (c) and (d) kernel average misorientation (KAM) maps of γ .

3.2. In-situ neutron diffraction of reverse transformation during annealing

The two-dimensional (2D) plots of the diffraction intensities of 111 γ , 200 γ and 110 α peaks are presented in Fig. 3(a) as a function of the annealing time. Diffraction profiles collected for 0.6 ks at the latter half of the isothermal holding at 1143 K and 1223 K after becoming a single γ phase are presented in Fig. 3(b). This corresponds to the EBSD results observed in Fig. 2. It was observed that both the diffraction peak intensity and full width at half maximum (FWHM) apparently decrease from 1143 K to 1223 K.

The detailed changes in diffraction intensities of some hkl peaks obtained in the axial direction are shown in Fig. 4. The plotted values were obtained by time slicing of every 60 s for the event-mode recorded data and all hkl peak intensities were normalized to the intensities at the beginning of 1093 K holding. The peak intensities are found drastically to decrease upon heating from 1160 K to 1200 K. The lowest indexed peak of 111 γ (at the largest wavelength) shows the most significant drop in peak intensity (larger than 50%) while the drop in higher indexed peak like 311 γ is small, in which the large scatters is due to its low absolute diffraction intensity. Kabra, *et al.* observed the similar decreasing and

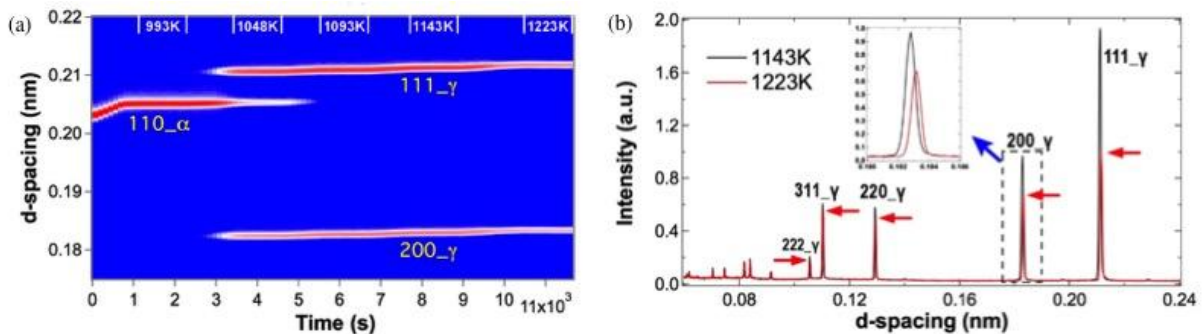


Fig.3 Neutron diffraction profile obtained during annealing: (a) 2D plots for austenite 111 and 200 and ferrite 110 peaks as a function of annealing time and (c) diffraction profiles collected within 0.6 ks at the latter half stage of isothermal holding at 1143 and 1223 K.

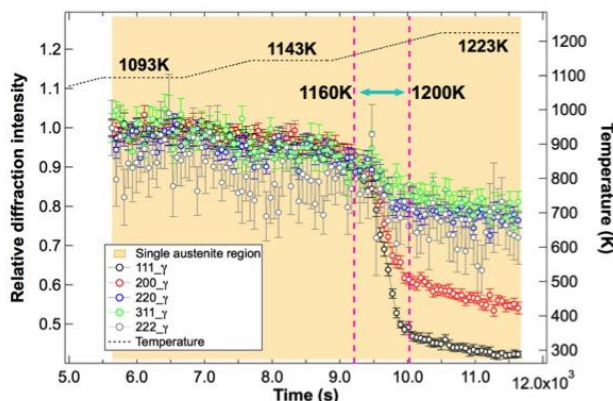


Fig.4 Changes in relative hkl diffraction intensities with heating after austenite reversion.

explained by the effect of primary extinction of the incident beam [9]. They have claimed that the increasing of crystal perfection driven by thermal recovery brings a transition from the kinematic to the dynamic theory of diffraction. Hence, the results in Fig. 4 must be caused by primary extinction of the incident beam at elevated temperatures related to the growth of type B grains which contain very small dislocation density (small KAM value). It would be concluded that the γ structure yielded by the growth of type A grains contain high density of sub-boundaries (dislocations array) which provide the driving force for the growth of type B grains. This phenomenon was similar to recrystallization.

4. SUMMARY

The microstructure evolution during reverse transformation at a slow heating rate in a Cr-Ni-Mo steel was investigated. *In-situ* observations at high temperatures during annealing demonstrated the formation of reversed austenite and grain refinement behavior. The features of the reversed austenite can be categorized into two types, A and B. The austenite grain memory phenomenon must be observed when the nucleation and growth of type A grains is more dominant than those of type B grains. The reversed austenite obtained from the type-A grains contain a high density of sub-grain boundaries that are the driving force for the growth of type-B grains, leading to a recrystallization-like phenomenon.

Acknowledgements: The authors sincerely thank Dr. T.Fukino from TSL solutions Co., for his help in *in-situ* EBSD experiment. *In-situ* diffraction experiment was performed at MLF J-PARC through project #2015A0129.

REFERENCES

- [1] T. Hara, N. Maruyama, Y. Shinohara, H. Asahi, G. Shigesato, M. Sugiyama and T. Koseki: *ISIJ Int.*, 49 (2009), 1792-1800.
- [2] S. Matsuda and Y. Okamura: *Trans. Iron Steel Inst. Jpn.*, 14 (1974), 444-449.
- [3] S. Matsuda and Y. Okamura: *Trans. Iron Steel Inst. Jpn.*, 14 (1974), 363-368.
- [4] S. Watanabe and T. Kunitake: *Trans. Iron Steel Inst. Jpn.*, 16 (1976), 28-35.
- [5] S. T. Kimmins and D. J. Gooch: *Met. Sci.*, 17 (1983), 519-532.
- [6] N. Nakada, T. Tsuchiyama, S. Takaki and S. Hashizume: *ISIJ Int.*, 47 (2007), 1527-1532.
- [7] N. Nakada, R. Fukagawa, T. Tsuchiyama, S. Takaki, D. Ponge and D. Raabe: *ISIJ Int.*, 53 (2013), 1286-1288.
- [8] N. Nakada, Tsuchiyama, S. Takaki, D. Ponge and D. Raabe: *ISIJ Int.*, 53 (2013), 2275-2277.
- [9] S. Kabra, K. Yan, D.G. Carr, R.P. Harrison, R.J. Dippenaar, M. Reid and K. Liss: *J. Appl. Phys.*, 113 (2013), 063513-1-063513-8.